Single-Molecule Magnets: Different Rates of Resonant Magnetization Tunneling in Mn_{12} Complexes**

Daniel Ruiz, Ziming Sun, Belen Albela, Kirsten Folting, Joan Ribas,* George Christou,* and David N. Hendrickson*

There is considerable and growing interest in single-molecule magnets.[1] A single-molecule magnet has a large-spin ground state with appreciable magnetic anisotropy, resulting in a barrier for reversal of the direction of magnetization. At low temperatures magnetization hysteresis loops are seen, as are out-of-phase ac susceptibility signals. The most thoroughly studied single-molecule magnet is **1**,[2–7] commonly called "Mn_{12}–acetate" or simply "Mn_{12}". In

$[Mn_{12}O_{12}(O_2CMe)_{16}(H_2O)_4]\cdot 2HO_2CMe\cdot 4H_2O$ **1**

addition to an application as a molecular memory device, interest in these molecular magnets stems from the possibility of observing macroscopic quantum tunneling (MQT).[8] Friedman et al.[9] reported for the first time the observation of resonant magnetization tunneling for Mn_{12}–acetate molecules in a crystal. Steps were observed at regular intervals of magnetic field in the magnetization hysteresis loop for oriented crystals. This has been confirmed by others.[10, 11] Herein we present magnetization hysteresis data for several $[Mn_{12}O_{12}(O_2CR)_{16}(H_2O)_4]$ complexes with different carboxylate ligands. Data are presented for oriented crystal samples. The hysteresis step heights are highly dependent on the substituent R. Thus, the rate of resonant magnetization tunneling varies appreciably from complex to complex.

Two new Mn_{12} complexes with the composition $[Mn_{12}O_{12}(O_2CR)_{16}(H_2O)_4]$, where R is either C_6H_4-2-Cl (**2**) or C_6H_4-2-Br (**3**), were prepared. As confirmed by the X-ray structure analysis,[12] complex $\mathbf{2}\cdot CH_2Cl_2\cdot 5H_2O$ possesses a $[Mn_{12}(\mu_3\text{-}O)_{12}]$ core comprising a central $[Mn^{IV}_4O_4]^{8+}$ cubane held within a nonplanar ring of eight Mn^{III} ions by eight μ_3-O^{2-} ions (Figure 1).

$[Mn_{12}O_{12}(O_2CC_6H_4\text{-}2\text{-}Cl)_{16}(H_2O)_4]$ **2**

$[Mn_{12}O_{12}(O_2CC_6H_4\text{-}2\text{-}Br)_{16}(H_2O)_4]$ **3**

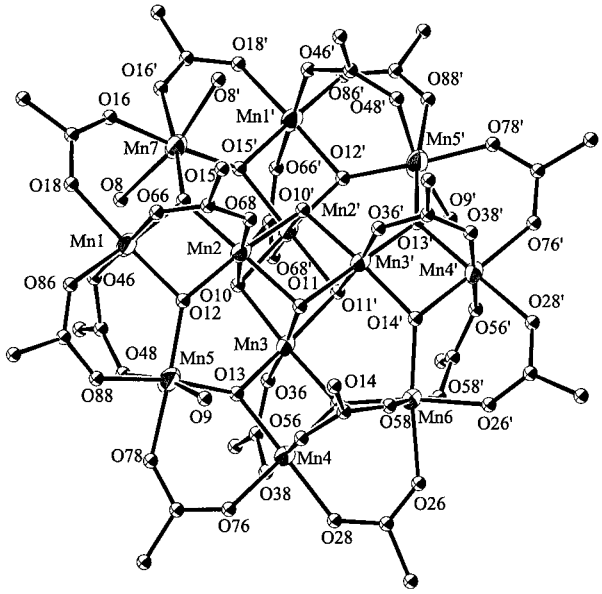

Figure 1. Structure of the core of $\mathbf{2}\cdot CH_2Cl_2\cdot 5H_2O$. The 2-chlorobenzoate rings are omitted for clarity.

Peripheral ligation of complex **2** is provided by sixteen η^2-μ-carboxylate groups and four H_2O ligands. Complex **2** is structurally similar to complex **1**. The most notable difference is the positioning of the four H_2O ligands: The acetate complex **1** has one H_2O ligand on each of four Mn^{III} ions. Complex **2** has one H_2O ligand [O9] on each of the two atoms labeled Mn5; the other two H_2O ligands [O8] are disordered together with the carboxylate oxygen atom that is shared by Mn1, Mn5, and Mn7. Complex **2** is located on a twofold axis, whereas complex **1** has a higher 2,2,2 crystal site symmetry. A variety of data, including variable-field magnetization, indicate complex **3** also has the same basic Mn_{12} core as **1** and **2**.

Magnetization hysteresis data obtained for oriented crystal samples of complexes **1**, **2,** and **3** at 2.0 K are shown in Figure 2. In each case, a few small crystals of a complex were suspended in eicosane held at 40 °C. This eicosane suspension was then introduced into a 5.5 T field, whereupon the crystals were oriented, each with their easy axis (i.e. the direction of the largest component of the crystal's magnetic susceptibility tensor) parallel to the field. The eicosane was then cooled to room temperature, which resulted in a solid wax cube with the crystals oriented with parallel easy axes. After thermal equilibration at 2.0 K, each sample was saturated in a field of +2.5 T. Then, the field was swept down to −2.5 T, and subsequently cycled back to +2.5 T. Each hysteresis loop was collected in a period of 1.5 h.

Steps are seen in the hysteresis loops for all three Mn_{12} complexes. The positions of the steps are highlighted by Figure 3, which shows the first derivative plots for the three hysteresis loops. Such steps in a hysteresis loop have been

[*] Prof. Dr. J. Ribas, Dr. B. Albela
Departament de Quimica Inorganica
Universitat de Barcelona
Diagonal, 647, E-08028-Barcelona (Spain)
Fax: Int. code + (34) 3490-7725
E-mail: jribas@kripto.qui.ub.es
Prof. Dr. G. Christou, Dr. K. Folting
Department of Chemistry
Indiana University
Bloomington, IN 47405-4001 (USA)
Fax: Int. code + (1) 812855-2399
E-mail: christou@indiana.edu
Prof. Dr. D.N. Hendrickson, Dr. D. Ruiz, Z. Sun
Department of Chemistry-0358
University of California at San Diego
La Jolla, CA 92093-0358 (USA)
Fax: Int. code + (1) 619534-5383
E-mail: dhendrickson@ucsd.edu

[**] This work was supported by the U.S. National Science Foundation. D.R. is grateful to the Spanish Ministry of Education for a postdoctoral fellowship. B.A. is grateful to the Spanish Ministry of Education for a doctoral fellowship. J.R. thanks the Dirección General de Investigación Científica y Técnica for financial support.

  1433-7851/98/3703-0300 $ 17.50+.50/0

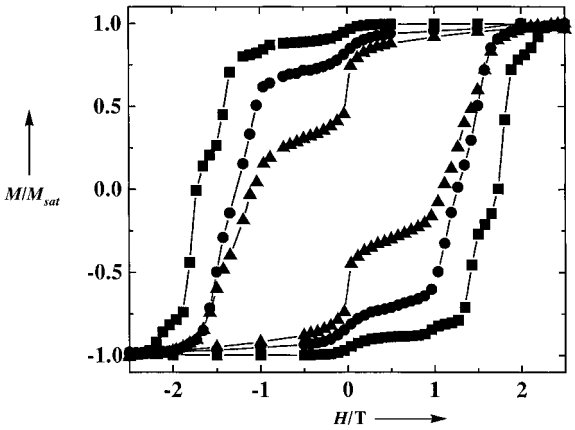

Figure 2. Magnetization hysteresis loops measured at 2.0 K for oriented crystals in eicosane matrix for three complexes: (■) acetate complex **1**; (●) 2-bromobenzoate complex **3**; (▲) 2-chlorobenzoate complex **2**. The magnetization data for each complex is plotted as a normalized value relative to the saturation magnetization M_{sat} for the complex.

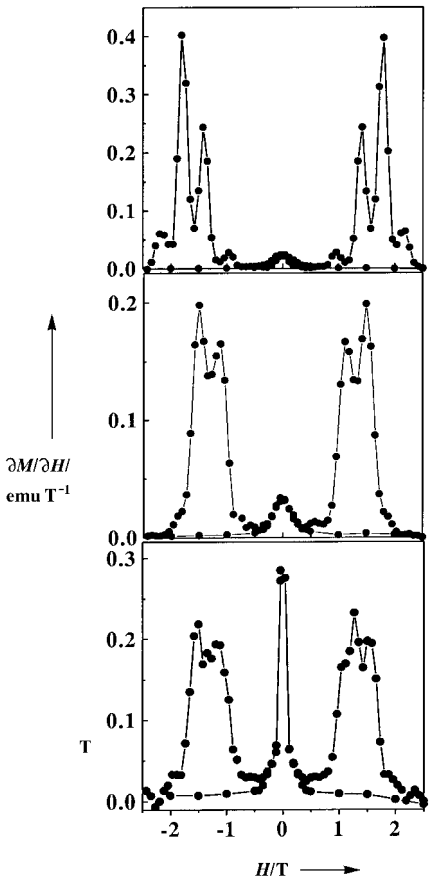

Figure 3. First derivative plots corresponding to the 2.0 K magnetization hysteresis loops shown in Figure 2. Top: acetate complex **1**; middle: Mn_{12}-2-bromobenzoate complex **3**; bottom: Mn_{12}-2-chlorobenzoate complex **2**.

shown[9–11] to be due to increases in the rate of change of the magnetization resulting from resonant magnetization tunneling. The relatively large ground-state spin of $S = 10$ together with considerable *negative* magnetic anisotropy for each molecule gives the double-well potential-energy diagram shown in Figure 4. The double well represents the change in

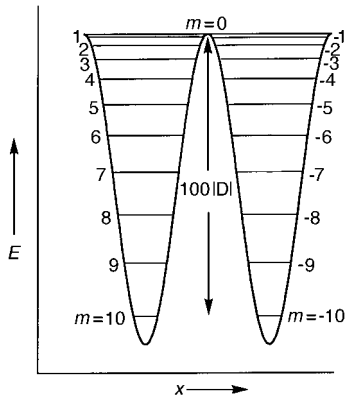

Figure 4. Plot of potential energy versus the magnetization direction for a single molecule with a $S = 10$ ground state. The axial zero-field interaction (DS_z^2) splits the $S = 10$ state into $m = \pm 10,\ \pm 9, \cdots \pm 1, 0$ levels. The barrier height U is equal to $|D|S^2 = 100\ |D|$ for the thermally activated process that involves converting the magnetic moment of the molecule from the "spin up" $m_s = 10$ level to the "spin down" $m_s = -10$ level. The diagram is drawn for zero applied field. x = Magnetization direction.

potential energy as a Mn_{12} molecule converts from the spin up to the spin down state. The application of a magnetic field stabilizes one state (e.g., $m_s = -10$) relative to the other. All of the Mn_{12} molecules populate the $m_s = -10$ when the sample is saturated in a large magnetic field. In sweeping out a hysteresis loop the first step occurs at zero field when there is an alignment of energy levels in the two parts of the double-well potential. At this point there is a resonant quantum mechanical tunneling. Additional steps are seen as the field is reversed and increased to give another alignment of levels in the two wells. Regularly spaced steps are seen[9–11] at temperatures lower than 2.0 K.

As can be seen in Figures 2 and 3, there are appreciable differences in the step heights between complexes **1**, **2,** and **3**. The scan rate and number of data points are the same for each of the three complexes. Thus, as the field is swept from +2.5 T to zero field, the first step seen for the acetate complex **1** is small. Complex **3** shows a steeper step at zero field. The steepest step is seen for complex **2**. Exactly what factors influence the rate of quantum tunneling of magnetization in these molecules is not known.[9–11] It is clear that a transverse (i.e., perpendicular to easy axis) magnetic anisotropy is needed, and this could arise from transverse quartic zero-field interactions[13] or from transverse magnetic fields caused by the nuclear spins.[14] Tunneling may not in fact occur between the lowest energy levels (e.g., $m_s = +10$ and -10 in zero field), but instead an Orbach process may be involved.[4] In this case, phonons are absorbed by a Mn_{12} molecule in a crystal exciting the molecule to a higher energy level from which it can tunnel through and/or be thermally excited over the barrier. The very appreciable differences seen in the zero-field steps for complexes **1**–**3** demonstrate a significant dependence of the observed tunneling behavior on the complex identity, and such studies should ultimately give insight about the mechanism of the tunneling; this information would be essential if the potential application of single-molecule magnets to, for example, memory devices is to be realized.

  1433-7851/98/3703-0301 $ 17.50+.50/0

Experimental Section

Samples of complex **1** were synthesized as previously described.[15]

$[Mn_{12}(\mu_3\text{-}O)_{12}(\mu\text{-}RCOO)_{16}(H_2O)_4]$, R = C_6H_4-2-Cl, C_6H_4-2-Br: A slurry of $[Mn_{12}(\mu_3\text{-}O)_{12}(\mu\text{-}MeCOO)_{16}(H_2O)_4]$ (0.50 g, 0.25 mmol) in CH_2Cl_2 (50 mL) was treated with an excess of the corresponding carboxylic acid RCOOH (8.0 mmol). The mixture was stirred overnight in a closed flask and filtered to remove any undissolved solid. Hexanes were added to the filtrate until precipitation of a dark brown solid was observed. The resulting solid was collected by filtration and the above treatment was repeated. The resulting filtrate was layered with hexanes (100–150 mL) and stored at room temperature for several days. Since the acid was highly soluble in diethyl ether but the Mn_{12} complex was only partially soluble in this solvent, a diethyl ether/hexane(s) mixture (1:4) was used to wash the resulting solid, which was finally dried in air. Recrystallization from CH_2Cl_2/hexane(s) gave crystals of complex **2** suitable for X-ray structure analysis. Complex **2:** Elemental analysis calcd for $[Mn_{12}O_{12}(O_2CC_6H_4\text{-}2\text{-}Cl)_{16}(H_2O)_4]\cdot 4H_2O$, $C_{112}H_{80}O_{52}Cl_{16}Mn_{12}$: C 38.58, H 2.30, Cl 16.30; found: C 38.4, H 2.4, Cl 16.2%. FT-IR (KBr): $\tilde{\nu}$ = 1589, 1560, 1544, 1519, 1473, 1412, 1164, 1054, 750, 725, 702, 651, 614, 552, 522 cm^{-1}. Complex **3:** Elemental analysis calcd for $[Mn_{12}O_{12}(O_2CC_6H_4\text{-}2\text{-}Br)_{16}(H_2O)_4]\cdot 3H_2O$, $C_{112}H_{78}O_{51}Br_{46}Mn_{12}$: C 32.17, H 1.88, Br 30.64; found: C 32.1, H 1.9, Br 30.7%. FT-IR (KBr): $\tilde{\nu}$ = 1585, 1543, 1518, 1470, 1411, 1161, 1045, 1028, 747, 695, 644, 614, 552, 518 cm^{-1}.

Received: August 11, 1997 [Z 10800 IE]
German version: *Angew. Chem.* **1998**, *110*, 315–318

Keywords: magnetic properties · manganese · single-molecule magnets · tunneling

[1] B. Schwarzschild, *Physics Today* **1997**, January 17; E. M. Chudnovsky, *Science* **1996**, *274*, 938.
[2] H. J. Eppley, H.-L. Tsai, N. De Vries, K. Folting, G. Christou, D. N. Hendrickson, *J. Am. Chem. Soc.* **1995**, *117*, 301.
[3] R. Sessoli, D. Gatteschi, A. Caneschi, M. A. Novak, *Nature* **1993**, *365*, 141; D. Gatteschi, A. Caneschi, L. Pardi, R. Sessoli, *Science* **1994**, *265*, 1054.
[4] M. A. Novak, R. Sessoli in *Quantum Tunneling of Magnetization—QTM'94* (Eds: L. Gunther, B. Barbara), Kluwer, Dordrecht, **1995**, pp. 189–207.
[5] R. Sessoli, H.-L. Tsai, A. R. Schake, S. Wang, J. B. Vincent, K. Folting, D. Gatteschi, G. Christou, D. N. Hendrickson, *J. Am. Chem. Soc.* **1993**, *115*, 1804.
[6] A. L. Burion, N. V. Prokof'ev, P. C. E. Stamp, *Phys. Rev. Lett.* **1996**, *76*, 3040.
[7] F. Lionti, L. Thomas, R. Ballou, B. Barbara, A. Sulpice, R. Sessoli, D. Matteschi, *J. Appl. Phys.* **1997**, *81*, 4608.
[8] D. P. Di Vincenzo, *Physica B* **1994**, *197*, 109; D. Loss, D. P. Di Vincenzo, G. Grinstein, D. D. Awschalom, J. F. Smyth, *ibid.* **1993**, *189*, 189.
[9] J. R. Friedman, M. P. Sarachik, J. Tejada, R. Ziolo, *Phys. Rev. Lett.* **1996**, *76*, 3830.
[10] L. Thomas, F. Lionti, R. Ballou, D. Gatteschi, R. Sessoli, B. Barbara, *Nature* **1996**, *383*, 145.
[11] J. Tejada, R. F. Ziolo, X. X. Zhang, *Chem. Mater.* **1996**, *8*, 1784.
[12] Crystal data for $[Mn_{12}O_{12}(O_2CC_6H_4\text{-}o\text{-}Cl)_{16}(H_2O)_4]\cdot(CH_2Cl_2)\cdot 5(H_2O)$ (complex **2**): $C_{113}H_{82}Cl_{18}Mn_{12}O_{56}$, noncentrosymmetric space group *Pnn*2, $T = -175\,^{\circ}C$, $a = 18.033(3)$, $b = 22.752(4)$, $c = 17.319(3)$ Å, $V = 7105.62$, $Z = 2$, $6.0^{\circ} \le 2\theta \le 45^{\circ}$. There were 4197 unique reflections with 3702 unique reflections with $F > 2.33\sigma(F)$; $R(F) = 0.0880$; $R_w(F) = 0.0872$. Several of the 2-chlorobenzoate ligands exhibited disorder in the position of the chlorine atom. The CH_2Cl_2 and five H_2O solvate molecules were present at about 50% occupancy. Crystallographic data (excluding structure factors) for the structure reported in this paper have been deposited with the Cambridge Crystallographic Data Centre as supplementary publication no. CCDC-100605. Copies of the data can be obtained free of charge on application to CCDC, 12 Union Road, Cambridge CB2 1EZ, UK (Fax: int. code + (44) 1223 336-033; e-mail: deposit@ccdc.cam.ac.uk).
[13] A. L. Barra, D. Gatteschi, R. Sessoli, *Phys. Rev. B*, in press.
[14] P. Polito, A. Rettori, F. Hartmann-Boutron, J. Villain, *Phys. Rev. Lett.* **1995**, *75*, 537; A. Garg in *Quantum Tunneling of Magnetization—QTM'94* (Eds.: L. Gunther, B. Barbara); Kluwer, Dordrecht, **1995**, pp. 273–287. A. Garg, *Phys. Rev. B* **1995**, *51*, 15161.
[15] T. Lis, *Acta Crystallogr. Sect. B* **1980**, *36*, 2042.

β-Homoalanyl PNAs: Synthesis and Indication of Higher Ordered Structures**

Ulf Diederichsen* and Harald W. Schmitt

Peptide nucleic acids (PNAs) are oligomers possessing a polyamide backbone in which the nucleobases of DNA/RNA function as recognition units. The interaction of PNAs with DNA double strands or RNA have increased in importance because of their potential use in antigene or antisense therapy.[1] In contrast, helical[2] or linear PNA–PNA self-pairing complexes[3] are uncharged models that are appropriate for investigating interactions between nucleobases or between nucleobases and amino acids[4] and for examining intercalation.[5] The linearity of two complementary strands is an important structural feature of our previous investigations on α-alanyl and α-homoalanyl PNAs. It is based on the 3.6-Å distance between two consecutive amino acid side chains in the β-sheet conformation, which is similar to the stacking distance of base pairs in DNA. Here we describe the synthesis of Boc-β-homoalanyladenine (**1**) and its oligomerization to β-PNAs. UV and CD spectra suggest that the hexamer and pentamer are self-organized in higher ordered structures, which can be rationalized from model studies as being structurally inevitable.

Although there are many methods to synthesize β-amino acids[6], nucleo-β-amino acids have not been described to date. The following difficulties have to be considered in linking the nucleobase to the γ position of the side chain (Scheme 1): 1) Nucleobases are poorly soluble in most organic solvents. 2) The desired nucleophilic attack by the *N*9 nitrogen atom of

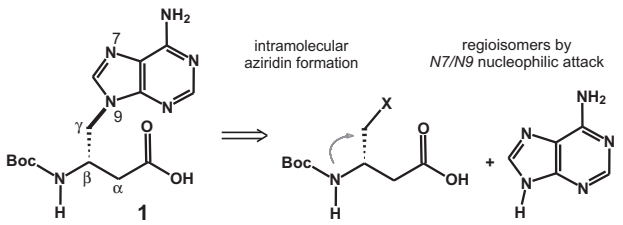

Scheme 1. Side reactions in the synthesis of nucleo-β-amino acid **1**.

[*] Dr. U. Diederichsen, H. W. Schmitt
Institut für Organische Chemie und Biochemie der
Technischen Universität München
Lichtenbergstrasse 4, D-85747 Garching (Germany)
Fax: Int. code + (49) 89 2891-3210
E-mail: ud@linda.org.chemie.tu-muenchen.de

[**] This work was supported by the Hermann-Schlosser-Stiftung (Ph.D. fellowship for H.W.S.) and the Deutsche Forschungsgemeinschaft (Di 542 2-1). We are grateful to Professor H. Kessler, Garching, for generous support.

